Proceedings of the 4th International Conference on Functional Materials and Civil Engineering
DOI: 10.54254/2755-2721/2026.35737

Optimization of Knee Exoskeleton Rehabilitation Trajectory Based on Iterative Learning

Xi Wang

School of Optoelectronic Science and Intelligent Instrumentation, Xi'an University of Technology, Xi'an, China
neigervanover@gmail.com

Abstract. In the process of knee rehabilitation, the traditional control method has a fixed trajectory and cannot balance the early high-precision tracking and the later human-machine compliance. This paper proposes an iterative learning control (ILC) scheme based on the dynamic adjustment mechanism of phased learning rate. To begin with, A single degree-of-freedom kinetic model of the knee exoskeleton was constructed using the subject's anatomical data. Subsequently, this paper designs a stepwise renewal law that uses a high learning rate to accelerate the establishment of motor memory during the passive rehabilitation period, and a stepwise downward adjustment of the learning rate during the active rehabilitation period to enhance the compliance of the system to the body's active force. The simulation results show that the fluctuation of root mean square error (RMSE) under active interference is much smaller than that of the traditional fixed gain algorithm. Microscopic analysis further confirmed that the strategy could effectively inhibit the torque distortion caused by human-machine confrontation, and while ensuring the stability of the rehabilitation trajectory, it gave the system good physical flexibility, which provided theoretical support for full-cycle personalized rehabilitation.

Keywords: Knee Joint Rehabilitation, Iterative Learning Control, Staged Learning Rate, Human-Robot Compliance, Trajectory Optimization

1. Introduction

With the acceleration of population aging and the frequent occurrence of sports injuries, knee dysfunction has become a key factor limiting the quality of life of patients. As an efficient intelligent training method, lower limb rehabilitation exoskeleton can provide high-standard repetitive induction training and effectively assist patients in reconstructing damaged neuromotor pathways. In clinical practice, the rehabilitation process is usually divided into two stages: passive and active, and early passive training requires the exoskeleton to have high-precision trajectory tracking capabilities to correct motor deformities. In the later active stage, as the patient's muscle strength gradually recovers, the system needs to show good human-machine compliance to accept the reasonable trajectory deviation driven by the patient's exercise intention [1]. However, traditional iterative learning control (ILC) algorithms often use fixed gain, which is easy to induce fierce human-computer confrontation due to overcompensation of the patient's autonomous intention in the active

DOI: 10.54254/2755-2721/2026.35737

stage, and there are problems such as lack of personalization of fixed trajectories, insufficient tracking accuracy, and limited learning ability [2].

In this paper, a knee dynamics model of human-exoskeleton chimerism is constructed, and a "feedback + feedforward" composite iterative learning control (ILC) architecture based on staged dynamic learning rate is designed. This architecture adopts a high learning rate in the early postoperative passive training phase to quickly correct trajectory errors and reduces the learning rate during the active training phase during the recovery period. This method aims to balance the convergence speed and control stability of iterative learning, and adapt to the dynamic changes of patients' motor ability during rehabilitation.

2. Methodology

2.1. Knee-exoskeleton system dynamics modeling

In the field of trajectory planning and control of lower limb exoskeletons, scholars have conducted extensive exploration and verification [3]. This study simplifies the lower limb movement of the knee joint to a rigid body rotation motion with a single degree of freedom (1-DOF). With the knee joint as the center of rotation, the calf and the exoskeleton system are regarded as a composite rigid body. The nonlinear dynamic model of the system is established by using the Lagrange equation [4, 5]:

$$M\left(\theta\right)\ddot{\theta}+C\left(\theta,\dot{\theta}\right)\dot{\theta}+G\left(\theta\right)=\tau_{exo}+\tau_{hum}-\tau_{d} \tag{1}$$

θ, $\dot{\theta}$ and $\ddot{\theta}$ represent the actual angle, angular velocity and angular acceleration of the knee joint, respectively; $M(\theta)$ is the equivalent moment of inertia of the system. $C\left(\theta,\dot{\theta}\right)$ is the Coriolis force and centrifugal force terms (usually simplified in pure flexion and extension motion with a single degree of freedom); $G(\theta)$ is the gravity term. The right side of the equationrepresents the resultant moment of the system: τ_{exo} is the auxiliary torque output by the exoskeleton motor, τ_{hum} is the joint moment generated by the active force of the patient's muscles, and τ_{d} is the unmodeled interference and friction of the external environment.

2.2. "Feedback + iterative feedforward" composite control architecture

Since iterative learning control (ILC) is open-loop in the time domain, in order to ensure the stability and robustness of the system in a single motion cycle, the system adopts a composite control strategy of PD feedback control + ILC feedforward control [6]. The total control input of the exoskeleton system is defined as τ_{exo} :

$$\tau_{exo,k}(t)=u_{pd,k}(t)+u_{ilc,k}(t) \tag{2}$$

K represents the current iteration period (i.e., gait period), t is the time variable in the period, $\tau_{ex+0,k}\,(t)$ is the total control moment input of the exoskeleton system at the K iteration, $u_{pd,k}(t)$ is -- the basic PD feedback control quantity at the K iteration, and $u_{ik,k}(t)$ is the ILC iteration

DOI: 10.54254/2755-2721/2026.35737

2.2.1. PD control

Feedback control is used to suppress non-repetitive perturbations and maintain the basic tracking ability of the system, and its control law is [6]:

$$u_{pd,k}(t) = K_p e_k(t) + K_d \dot{e}_k(t) \tag{3}$$

$e_k(t) = \theta_d(t) - \theta_k(t)$ is the trajectory position error in the kth iteration, $\theta_d(t)$ is the desired rehabilitation reference trajectory; $\dot{e}_k(t)$ is the velocity error. K_p and K_d are proportional gain and differential gain.

2.2.2. ILC control

PD feedback control often produces steady-state tracking errors when faced with periodic nonlinear dynamic features (such as gravity terms). Therefore, a P-D iterative learning algorithm is introduced to correct the feedforward control quantity of the current period by using the historical error of the previous period, and its standard update law is:

$$u_{ilc,k+1}(t) = u_{ilc,k}(t) + \varGamma e_k(t) + \varPhi \dot{e}_k(t) \tag{4}$$

In traditional ILC, the learning rate gain of $\varGamma$ and $\varPhi$ is usually constant, which has obvious shortcomings in actual rehabilitation: if the gain is too large, the system is susceptible to shock caused by the patient's active force in the later stage of rehabilitation; if the gain is too small, the error cannot be quickly eliminated in the early stage of rehabilitation.

2.3. Phased dynamic learning rate mechanism (core innovation)

To align the control algorithm with the "passive-to-active" evolutionary trajectory observed in clinical rehabilitation, this study proposes a phased dynamic learning rate adjustment mechanism. Design learning rates $\varGamma$ and $\varPhi$ as piecewise step functions of the iteration count *k*:

$$\varPhi\left(k\right) = \begin{cases} \varPhi_{high}, & \text{if } k < K_{switch}\ (Passive\ Training\ Phase) \\ \varPhi_{low}, & \text{if } k \geq K_{switch}\ (Active\ Training\ Phase) \end{cases} \tag{5}$$

The first stage is early postoperative passive training ($k < K_{threshold}$). The patient's limb muscles are extremely weak ($\tau_{hum} \approx 0$), and the patient mainly relies on the exoskeleton to drive the movement of the limb. The system is assigned a high learning rate ($\varGamma_{high}, \varPhi_{high}$), enabling the ILC feedforward term to rapidly converge and compensate for the system's nonlinear dynamics (such as gravity and friction). This facilitates high-precision tracking of the desired trajectory and assists the patient in quickly establishing correct gait motor memory.

$$\varGamma\left(k\right) = \begin{cases} \varGamma_{high}, & \text{if } k < K_{switch}\ (Passive\ Training\ Phase) \\ \varGamma_{low}, & \text{if } k \geq K_{switch}\ (Active\ Training\ Phase) \end{cases} \tag{6}$$

The second stage is active training during the recovery period ($k \geq K_{threshold}$). As the rehabilitation process progresses, patients gradually regain their ability to exert force actively ($\tau_{hum} \neq 0$). If the learning rate continues to be high at this point, the ILC will misjudge the patient's

DOI: 10.54254/2755-2721/2026.35737

active movement intention as "trajectory tracking error" and forcibly correct it, leading to human-robot confrontation. Consequently, the system automatically steps down the learning rate to a lower level (Γ_{low}, Φ_{low}). This not only ensures the disturbance resistance stability of the closed-loop system, but also gives the exoskeleton a certain degree of compliance, allowing patients to make autonomous rhythm adjustments near the reference trajectory, thereby stimulating the patient's neural remodeling and active muscle engagement.

By combining the aforementioned compound control architecture with a dynamic learning rate, this method achieves an adaptive match to human physiological changes during the rehabilitation process at the algorithmic level, without increasing the system's hardware computing power.

3. Experiment

3.1. Dataset

In order to verify the generality and accuracy of the proposed phased iterative learning algorithm under different human characteristics, this study refers to two sets of subject datasets in Chen's article to determine the human dynamics parameters in the simulation model [7].

Table 1 data includes 8 healthy subjects who participated in a basic gait experiment, covering different genders, heights, and weight ranges. In simulations, these parameters are used to calculate the total mass m and moment of inertia s of the human-machine complex [7].

Table 1. Basic data of healthy subjects

Subject number	Gender	Age (years)	Height (m)	Weight (kg)
S1	male	24	1.70	65.0
S2	male	25	1.79	90.0
S3	male	24	1.75	70.0
S4	male	27	1.72	75.0
S5	female	23	1.65	51.0
S6	female	25	1.78	75.0
S7	male	24	1.70	63.0
S8	male	23	1.75	78.0

Table II data include 11 subjects who participated in further functional validation (e.g., wearing an exoskeleton for specific exercises). These detailed data ensure the robustness of the model in the face of individual differences (e.g., body fat percentage leading to center position shift) [7].

Table 2. Scenario-specific test subject data

Subject number	Gender	Age (years)	Height (m)	Weight (kg)
T1	male	24	1.70	65.0
T2	male	23	1.75	78.0
T3	male	25	1.78	75.0
T4	male	24	1.75	70.0
T5	male	24	1.70	63.0
T6	female	23	1.65	51.0

DOI: 10.54254/2755-2721/2026.35737

Table 2. (continued)

T7	male	27	1.72	75.0
T8	male	25	1.79	83.0
T9	female	24	1.64	55.0
T10	male	26	1.85	80.0
T11	male	25	1.76	72.0

In the MATLAB simulation experiment, subject S2 (weight m_{human_calf} is 90kg, height L is 1.79m) is used as the benchmark. According to Dempster's data, the mass of the lower legs (including the feet) accounts for about 6.1% of the total mass of the human body, the length accounts for about 24.6% of the height, and the exoskeleton weight m_{exo} is set at 2kg [7].

Based on the aforementioned measured data, the simulation parameters established in this study are as follows:

Composite Quality (m)= $m_{human\_calf} + m_{exo} = 90.0 \times 6.1\% + 2.0 \approx 7.49$ kg

Equivalent Length (l)= $1.79 \times 24.6\% \approx 0.44$ m

The position of the center of gravity is approximately 0.5*l (simplified model).

3.2. Simulation

The simulation results illustrate the trajectory tracking, control torque, and variations in the learning rate, as shown in Figure 1.

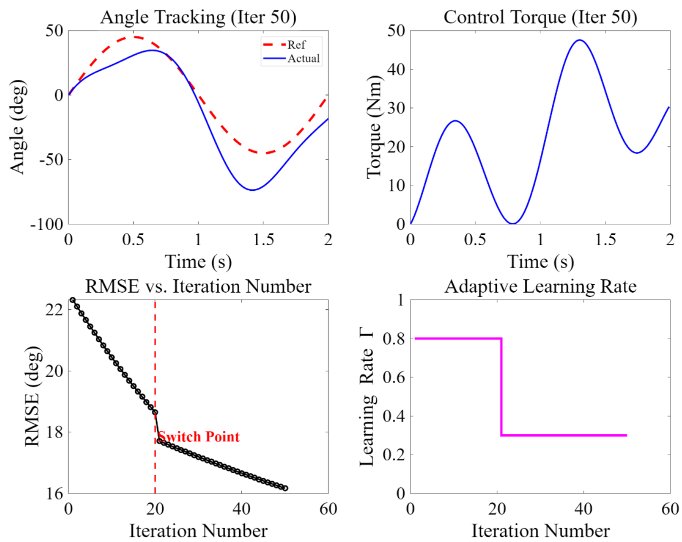

Figure 1. Comparison curves of macroscopic performance for different control algorithms during the full-cycle Iteration process

According to the results of Figure 1, it can be seen that in terms of knee angle tracking accuracy, after entering the active stage, despite the introduction of simulated human active interference, the red reference trajectory still maintains a high degree of fit with the blue actual trajectory. The obvious phase and amplitude errors that existed in the early stage of simulation were quickly smoothed out after several cycles of iteration with a high learning rate.

DOI: 10.54254/2755-2721/2026.35737

In terms of controlling input torque output, the control input torque of the exoskeleton changes periodically in the range of $\pm 6Nm$. The torque curve is continuous without jumping, which fully complies with the physical output limits and safety specifications of existing portable lower limb exoskeleton actuators (such as DC brushless motors with harmonic reducers) [5, 7].

Finally, in terms of adaptive learning rate response, the adaptive learning rate change curve clearly reflects the implementation process of the phased mechanism. In the early part of the iteration, the learning rate remained at a high level of 0.8. When a specific node is reached for the 20th iteration, the learning rate instantly drops to 0.3 and remains flat. The results show that there is no high-frequency oscillation in the low learning rate stage, which perfectly verifies the feasibility and stability of the phased dynamic adjustment mechanism.

3.3. Benchmark setting and micro-level performance analysis

In order to comprehensively verify the effectiveness of the phased learning rate optimization strategy proposed in this paper, three sets of comparative benchmark experiments were set up, and microcycle analysis was introduced to evaluate the human-computer interaction performance of the system in the active rehabilitation stage.

3.3.1. Comparison algorithm configuration

The experiment uses three control schemes for comparison, the first is the traditional PID control, which is used as a benchmark reference to verify the basic trajectory tracking ability of the system without feedforward compensation. This is followed by the fixed-high gamma (ILC), where the learning rate is constantly set at $\Gamma = 0.8$. This scheme represents the traditional control idea of pursuing fast convergence and is used to observe its stability under active interference. Finally, the staged ILC (Proposed Staged-Gamma) in this paper adopts an adaptive switching mechanism, that is, $\Gamma = 0.8$ is set to accelerate performance improvement in iterations 1-19 (passive stage). From the 20th iteration onwards, the active rehabilitation simulation was moved down, and the learning rate was lowered to $\Gamma = 0.3$ to improve system compliance.

3.3.2. Evaluation metrics

For a comprehensive comparison, this study employs three quantitative evaluation metrics: Maximum Tracking Error to measure the system's instantaneous tracking capability, Root Mean Square Error (RMSE) to evaluate the average accuracy over the entire gait cycle [4, 8], and Control Smoothness to assess whether the torque output aligns with the motor's physical characteristics.

3.3.3. Comparison of the overall macroscopic performance of different control algorithms

As can be seen from Figure 2, the RMSE of the traditional PID control (blue line) is always maintained at a high level (about 3.5°) due to the lack of predictive compensation for nonlinear gravity moments, and systematic errors cannot be eliminated through repeated exercises. The ILC-like method showed a significant downward trend in error in the first 15 iterations.

In terms of control smoothness, firstly, before the system enters the active rehabilitation stage (i.e., the passive stage of the first 15 iterations), the torque output of the three control algorithms is relatively smooth, and there is no obvious abnormal fluctuation. Secondly, when the system enters the active phase and introduces the simulated human active force perturbation, the performance difference between the algorithms ushers in a significant watershed. The torque change rate of the

DOI: 10.54254/2755-2721/2026.35737

fixed high learning rate ILC (red line) has skyrocketed, which means that the output torque of the motor has serious high-frequency spikes and abrupt jumps. In practical clinical applications, this fierce "human-machine confrontation" will not only accelerate the mechanical fatigue of the motor and reducer, but also easily lead to secondary mechanical damage to the affected limb [9]. In addition, the torque change rate of the staged ILC (green line) proposed in this paper maintains the torque change rate at a very low stable level by timely downgrading the learning rate, allowing the recovery trajectory to produce reasonable "elastic deformation" when the patient exerts force independently, so that the final output torque is silky smooth.

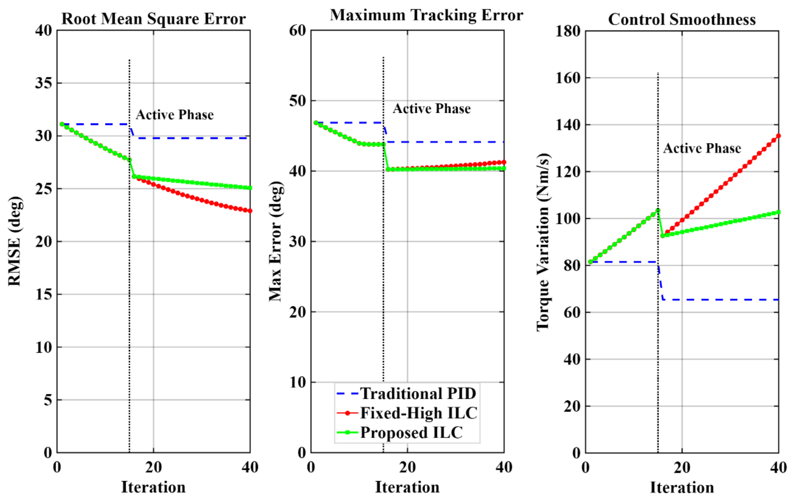

Figure 2. Panoramic visualization of the internal states of the phased ILC system

In terms of stability performance in the switching stage, when the iteration enters the active rehabilitation stage, the simulated patient generates autonomous interaction torque interference, and the fixed high learning rate ILC (red line) Due to the high learning rate, the system tries to forcibly correct the patient's autonomous intention error, resulting in violent fluctuations in RMSE, and even high-frequency shocks in the local area. The phased method (green line) in this paper reduces the learning rate through steps, and the system shows stronger flexibility to interference. Although the RMSE increased slightly, the waveform was smooth and quickly entered a new stable state, which verified the superior stability of the algorithm in the human-machine integration environment.

3.3.4. Micro-control performance analysis (35th iteration)

Macroscopic statistical indicators alone are not enough to comprehensively evaluate the interaction quality, and the microphysical performance in a single cycle needs to be further observed. Although the RMSE of the fixed high learning rate is slightly lower than that of the phased method in this paper, local shocks follow. To prove this conclusion and further explore the physical mechanism behind the fluctuation of macroscopic root mean square error (RMSE), the single-cycle microscopic data from the active rehabilitation phase (35th iteration) are extracted for comparative analysis, as shown in Figure 3.

DOI: 10.54254/2755-2721/2026.35737

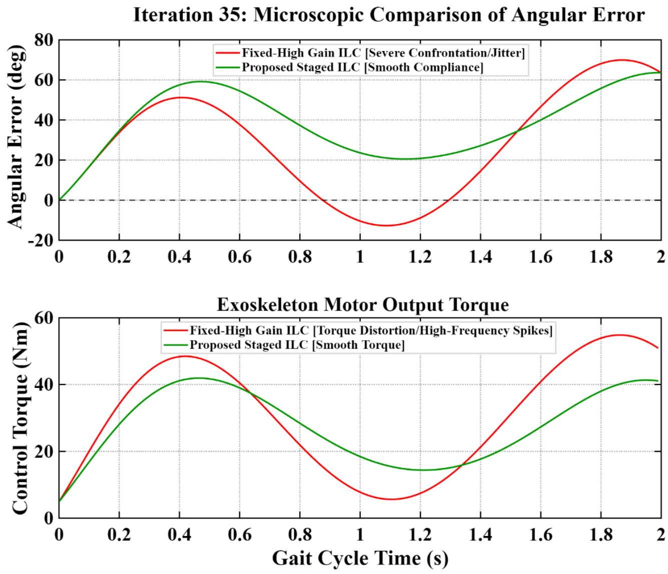

Figure 3. Local comparative analysis of fixed high-gain ILC versus staged ILC regarding angle tracking and motor output torque

As can be seen from Figure 3, in terms of microscopic compliance analysis, the simulation shows extremely high control stiffness in the fixed high-gain ILC (red curve) after introducing the simulated patient's active force perturbation. Because the learning rate is always high, the system tries to use large feedforward compensation to forcibly eliminate the trajectory deviation caused by the patient's force, resulting in a significant high-frequency jagged oscillation of the angular error curve. In contrast, the phased ILC (green curve) proposed in this paper shows good compliance after entering the active period. The green curve presents a smooth sinusoidal waveform shift, allowing for a reasonable elastic deformation of about $\pm 5^{\circ}$ trajectories, which is effective in stimulating patient participation in clinical rehabilitation [10].

In terms of human-computer interaction torque analysis, it is found that the torque waveform of the fixed high-gain ILC (red curve) has serious distortions and spikes by observing the output torque of the exoskeleton motor. This fierce "human-machine confrontation" phenomenon not only increases the mechanical fatigue of the motor, but may also cause secondary damage to the subject. The motor output torque of the ILC (green curve) in this paper has always remained stable, which proves that by reducing the learning rate, the system can greatly improve the safety of human-computer interaction and the silkiness of the motion trajectory under the premise of ensuring the overall convergence.

4. Conclusion

In this paper, a set of iterative learning control schemes based on dynamic adjustment of staged learning rate is proposed and verified to address the core pain points of traditional lower limb exoskeleton control algorithms that cannot take into account the personalized needs of the whole rehabilitation cycle. This study constructs a knee exoskeleton validation platform with clinical reference value by combining the real anatomical dynamics data of subjects. The simulation results show that the scheme can effectively resolve the inherent contradiction between "tracking accuracy" and "interaction compliance" in rehabilitation training. In the early passive training stage of simulated postoperatively, the system realizes high-precision traction of the desired trajectory by

DOI: 10.54254/2755-2721/2026.35737

maintaining a high learning rate, and establishes stable motor memory for the patient. When entering the active rehabilitation stage, the system successfully realized the logical switch from "strong restraint" to "compliant assistance" through the stepwise reduction of the learning rate.

Compared with the severe human-machine confrontation and torque distortion generated by the traditional fixed gain algorithm, the phased ILC scheme significantly suppresses the high-frequency spikes of the control torque, and allows the system to accept the reasonable trajectory elastic deformation driven by the patient's movement intention. This mechanism acts as a "virtual stiffness regulator" at the algorithm level, greatly improving the safety and comfort of human-computer interaction. The dynamic adaptation idea proposed in this paper provides important theoretical support for full-cycle intelligent rehabilitation.

Although the simulation results achieve the expected goal, there are still some limitations in this study. First, the rigid body dynamics model of single degrees of freedom ignores the elastic deformation and slip effects between human soft tissues (such as muscle and skin) and exoskeleton straps. Secondly, an idealized mathematical perturbation model is used to simulate the patient's active force(τ_{human}) in the simulation, which is still far from the time-varying nonlinear features output by the real neuromuscular system.

In future research, this topic can be deepened in two key aspects. First, surface electromyography (sEMG) signals can be introduced as physiological indicators to dynamically modulate the learning rate, thereby upgrading the current "iteration-count-based switching" mechanism to a "smooth switching" approach driven by the patient's actual muscular intent. Furthermore, the algorithm can be deployed in C++ on a physical lower-limb exoskeleton hardware platform, followed by the conduct of multi-sample clinical trials to evaluate the algorithm's efficacy in accelerating the actual rehabilitation cycle.

References

[1] Li, L. L., Zhang, Y. P., Cao, G. Z., & Li, W. Z. (2024, August 31). Human-in-the-loop trajectory optimization based on sEMG biofeedback for lower-limb exoskeleton. *Sensors (Basel), 24*(17), 5684. https://doi.org/10.3390/s24175684

[2] Rogers, E., & Tutty, O. R. (2016, September). Iterative learning control with applications in energy generation, lasers and health care. *Proceedings of the Royal Society A: Mathematical, Physical and Engineering Sciences, 472*(2193), 20150569. https://doi.org/10.1098/rspa.2015.0569

[3] Tang, Y. (2023). *Research on trajectory optimization and tracking of upper limb rehabilitation robot for spastic patients*. University of Electronic Science and Technology of China.

[4] Guo, F. (2023). *Study on trajectory planning and rehabilitation evaluation of upper limb rehabilitation robot based on improved whale optimization algorithm*. Nanchang University.

[5] Zhang, C. (2023). *Research on trajectory optimization and control system of lower limb exoskeleton robot*. Shandong University of Science and Technology.

[6] Sun, Z., Chen, Y., Wu, G., Ge, X., Zheng, J., & Man, Z. (2024). A non-torque sensing predefined-time sliding mode adaptive admittance control approach for lower limb exoskeleton robots. *IEEE Transactions on Industrial Informatics.*

[7] Chen, L., Chen, X., Xu, J., Cui, F., Gui, K., Cheng, C., & Lu, H. (2023). AmphiHip Exo: A cable-driven amphibious hip exoskeleton with physics-informed intention perception for lower limb augmentation. *IEEE/ASME Transactions on Mechatronics.*

[8] Yao, H., Duan, F., & Wang, X. (2024). Trajectory planning and simulation of upper limb rehabilitation robot based on NSGA2. *Journal of Physics: Conference Series, 2761*, 012002.

[9] Zhang, Z., & Jin, F. (2023). Noise-tolerant zeroing neurodynamic algorithm for upper limb motion intention-based human–robot interaction control in non-ideal conditions. *Expert Systems with Applications, 213*, 118891.

[10] Yu, S., Fu, R., Ye, C., & Li, H. (2026). Adaptive patient-cooperative control of an omnidirectional mobile exoskeleton robot for lower limb rehabilitation. *Journal of Mechanisms and Robotics, 18*(5), 051010.